Study of Si and Ge Atoms Termination Using H-Dilution in SiGe:H Alloys Deposited by Radio Frequency (13.56 MHz) Plasma Discharge at Low Temperature

Ismael Cosme [1,2,](ID), **Andrey Kosarev [1]**, **Saraí Zarate-Galvez [1]**, **Hiram E. Martinez [1]**,
Svetlana Mansurova [1] (ID) and **Yuri Kudriavtsev [3]**

[1] Instituto Nacional de Astrofísica, Óptica y Electrónica (INAOE), Luis Enrique Erro # 1, Tonantzintla,
Puebla 72840, Mexico; akosarev@inaoep.mx (A.K.); sarai.zarate@inaoep.mx (S.Z.-G.);
hiram@inaoep.mx (H.E.M.); smansur@inaoep.mx (S.M.)

[2] Consejo Nacional de Ciencia y Tecnología—INAOE, Luis Enrique Erro # 1, Tonantzintla,
Puebla 72840, Mexico

[3] Centro de Investigación y Estudios Avanzados (CINVESTAV), Departamento de Ingeniería Eléctrica,
Cinvestav IPN, Ciudad de Mexico 07360, Mexico; yuriyk@cinvestav.mx

* Correspondence: ismaelcb@inaoep.mx; Tel.: +52-222-266-31-00

Abstract: In this work, we present the study of the atomic composition in amorphous $Si_XGe_Y:H_Z$ films deposited by radio frequency (RF—13.56 MHz) plasma discharge at low deposition temperature. A study and control of Si and Ge atoms termination using H-dilution in SiGe:H alloys deposited by RF plasma discharge was conducted and we made a comparison with low-frequency plasma discharge studies. Solid contents of the main elements and contaminants were determined by SIMS technique. It was found that for low dilution rates from $R_H = 9$ to 30, the germanium content in the solid phase strongly depends on the hydrogen dilution and varies from $Y = 0.49$ to 0.68. On the other hand, with a higher presence of hydrogen in the mixture, the germanium content does not change and remains close to the value of $Y = 0.69$. The coefficient of Ge preferential incorporation depended on R_H and varied from $P_{Ge} = 0.8$ to 4.3. Also, the termination of Si and Ge atoms with hydrogen was studied using FTIR spectroscopy. Preferential termination of Si atoms was observed in the films deposited with low $R_H < 20$, while preferential termination of Ge atoms was found in the films deposited with high $R_H > 40$. In the range of $20 < R_H < 40$, hydrogen created chemical bonds with both Si and Ge atoms without preference.

Keywords: Alloys; silicon-germanium; hydrogen dilution; RF PECVD

1. Introduction

Silicon-germanium thin films ($Si_XGe_Y:H_Z$) deposited by Plasma Enhanced Chemical Vapor Deposition (PECVD) have been studied over the last decades regarding solar cell applications due to their reduced band-gap and their absorption in the infrared spectrum (IR) [1]. In recent years, silicon-germanium alloys have also demonstrated potential applications in new device concepts such as 3D structured devices [2–4], un-cooled micro-bolometers [5], microelectromechanical systems (MEMS) [6], and biomedical applications [7]. However, the increase of Ge content in these alloys is reported to deteriorate the electronic properties and the device characteristics. Then, better performance and stability requires much effort to improve the film quality.

One promising technique to improve the film quality of $Si_XGe_Y:H_Z$ alloys deposited by PECVD is the hydrogen dilution method [8,9]. Many groups have reported results obtained by this technique and

have discussed the role of hydrogen dilution for a relatively low hydrogen dilution ratio R_H in the range of less than $R_H = 20$ ($R_H = Q_{H2}/Q_{SiH4}$, where Q_{H2} is the hydrogen flow rate, and Q_{SiH4} is the silane flow rate) at substrate temperatures above 200 °C [10]. Most of the papers deal, however, with relatively low Ge concentration (Y < 0.5) and high deposition temperatures (Td > 200 °C) because these parameters provide films with optoelectronic properties acceptable for application in the device structures.

The investigation of $Si_XGe_Y:H_Z$ films over the entire range 0 < Y < 1 was systematically studied by our group for low frequency (LF) and high deposition temperature, and the results were reported in [9]. Good quality SiGe films were reported also for LF PECVD in references. [11–13]. On the other hand, the effect of dilution gas at low deposition temperatures (T_d < 200 °C) on both, film growth and electronic properties has not been systematically studied for standard radio frequency (13.56 MHz) conditions. However, nowadays thin films deposited at low temperatures (Td < 200 °C) are a requirement for novel device applications such as hybrid inorganic-polymer structures [14,15] and flexible substrates [16].

It should be noted that the problem of optimization of conditions for PECVD fabrication of semiconductor materials consisting of more than one semiconductor atom e.g., $Si_XGe_Y:H_Z$ is more complex than that for one semiconductor atom, e.g., Si:H. The deposition of hydrogenated alloys has two important aspects: (a) Incorporation of semiconductor atoms from the gas phase (typically preferential incorporation of one atom is observed with the preferential factor depending on the deposition conditions), and (b) hydrogen termination of both atoms, let us say Ge–H and Si–H; hydrogen termination is also realized with the preference of one atom for hydrogen termination. The latter has not been studied and therefore the optimal (from point of view electronic properties) hydrogen distribution between two atoms is unknown. Hydrogen dilution of the gas mixture used for semiconductor deposition has demonstrated a significant effect on deposition rate, atom incorporation from the gas phase into a solid-state, and as expected on hydrogen termination of both atoms.

This paper reports the composition and Si and Ge atoms termination in $Si_XGe_Y:H_Z$ films using hydrogen dilution in deposition under standard RF (13.56 MHz) PECVD at low deposition temperature (T_d = 160 °C) compatible with polymer semiconductor and flexible plastic substrates [17]. The effect of hydrogen dilution on growth, composition, and Si–H and Ge–H hydrogen bonding of high Ge content $Si_XGe_Y:H_Z$ (Y > 0.5) was studied.

2. Materials and Methods

The samples were fabricated using a cluster tool system from "MVSystem. Inc. (Denver, CO, USA)" in a standard capacitive PECVD chamber (see Appendix A, Figure A1). The R.F. electrode assembly consists of a dark shield, cathode- anode electrode configuration with a distance of 1.9 cm, and automatic matching. The gas injector contains multiple small holes and the location provides a uniform flow of gasses across the plasma region with a substrate area of 15.6 × 15.6 cm^2. SiGe:H films were deposited in the chamber after cleaning and passivation of the walls by the growth of intrinsic film, the background vacuum level was lower than 5×10^{-7} Torr and a leakage rate was $R_{leak} = 4.5 \times 10^{-4}$ sccm. Intrinsic SiGe:H films were deposited from (50% SiH_4 + 50% GeH_4) + H_2 mixture, all the gases used were semiconductor purity and were pre-mixed before introducing them to the chamber. The hydrogen dilution ratio was defined as $R_H = C_H/(C_{Si} + C_{Ge})$ where C_H is the concentration of hydrogen atoms, C_{Si} and C_{Ge} are the concentrations of Si and Ge atoms in the gas phase, respectively. Thus, R_H was varied from 9 to 80 by increasing the H_2 flow from $Q_{H2} = 9$ to 80 sccm at constant pressure P = 0.55 Torr. Deposition temperature was fixed at T_d = 160 °C and deposition time was set at t_d = 2000 s. RF discharge was excited at frequency f = 13.56 MHz with power W = 5 W (22 mW/cm^2). The substrates used were p$^+$-doped c-Si wafers for SIMS analysis. The experimental films were characterized by the measurements as follows: deposition rate, V_d, was obtained from step profile measurements of the silicon–germanium films with a "DektakXT profiler" (Bruker, Billerica, MA, USA). The deposition rate was calculated assuming that the film thickness is a linear function of time: $V_d = d/t_d$, where d is the film thickness and t_d is the deposition time.

Solid-phase atomic content in SiGe:H films was determined by Secondary Ion Mass Spectroscopy (SIMS) Technique. For this purpose, a time of flight TOF-SIMS-5 instrument from "ION TOF GmbH" (Muster, Germany) was used. The depth profiling was realized with a double beam regime: A pulsing Bi^+ ions beam was used for analysis, and low energy Cs^+ ions beam for a delicate sputtering. Both negative secondary ions and positive CsM^+ cluster ions (where M is the element of interest) were monitored in parallel measurements for dopants, contaminants (C, O, N, F), and the main components (Si, Ge, H) characterization. Quantification of intensity in experimental data was performed using the implanted standards and by measurements of reference SiGe compounds with a known composition.

H-termination characterization was performed, the infrared (IR) absorption spectra of the films were measured with an FTIR spectrometer from "Brucker Optics" (model "Vector-22", Ettingen, Germany) over the range 350–4000 cm^{-1}. The measured absorbance spectra were normalized to the absorbance spectrum of a crystalline silicon substrate, and the spectral absorption spectra were calculated. The spectra were analyzed systematically after baseline subtraction and computer deconvolution.

3. Results

3.1. Film Growth

After fabrication, the thickness of the films was measured by the profiler to calculate the deposition rate V_d. The deposition rate of film thickness is depicted in Figure 1 in comparison with that obtained from the measurements of the crater generated by SIMS measurements. $V_d(R_H)$ shows a reduction from $V_d = 1.2$ to 0.5 A/s with a change in R_H from $R_H = 9$ to 40 and only a small change (practically negligible) in the range $R_H = 40$ to 80. Comparing these V_d values with those reported in reference [9] for SiGe:H films deposited by low frequency (LF) PECVD and high temperature we noticed similar V_d values for low Ge content (about 0.1 in the gas phase) to those for RF PECVD films. On the other hand, values of the deposition rate of $V_d = 0.9 \pm 0.1$ Å/s are found in reference [18] for film growth with 0.5 Ge content in the gas phase. It is important to note that V_d behavior depends on the selection of experimental variables, here the hydrogen dilution provides lower deposition rates when it is raised. However, opposite behavior is found when the germanium content in gas phase C_G is taken as the variable e.g., the deposition rate increases from 1.5 to 3.7 Å/s for LF discharge [9] and from 4 to 11 Å/s for RF discharge when C_{Ge} is raised, for hydrogen dilution ratios of $R_H = 0.4$ and $R_H = 20$, respectively.
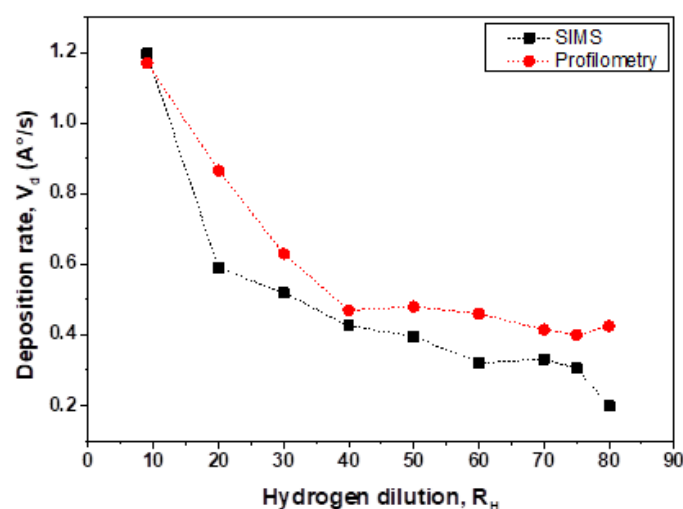

Figure 1. Deposition rate as a function of hydrogen dilution ratio $V_d(R_H)$ calculated from step measurements and estimation of depth from measurements of the crater created by SIMS.

3.2. Composition of the Films

A typical SIMS profile is shown in Figure 2 corresponding to a $Si_X Ge_Y:H_Z$ film deposited at hydrogen dilution $R_H = 30$. The main contaminant element is seen to be oxygen. However, the SIMS signal also contains a contribution from residuals in the analytical chamber of the SIMS instrument. The contents of Oxygen (O), Carbon (C), and Nitrogen (N) atoms in the solid films are around the level of $2.8 \pm 0.9 \times 10^{20}$, $4 \pm 1 \times 10^{19}$, and $1.40 \pm 0.05 \times 10^{19}$ atoms/cm^3, respectively. The reasons for relatively high contaminations are not clear at present and could be caused by both, deposition processes and/or vacuum conditions in the SIMS measurements.
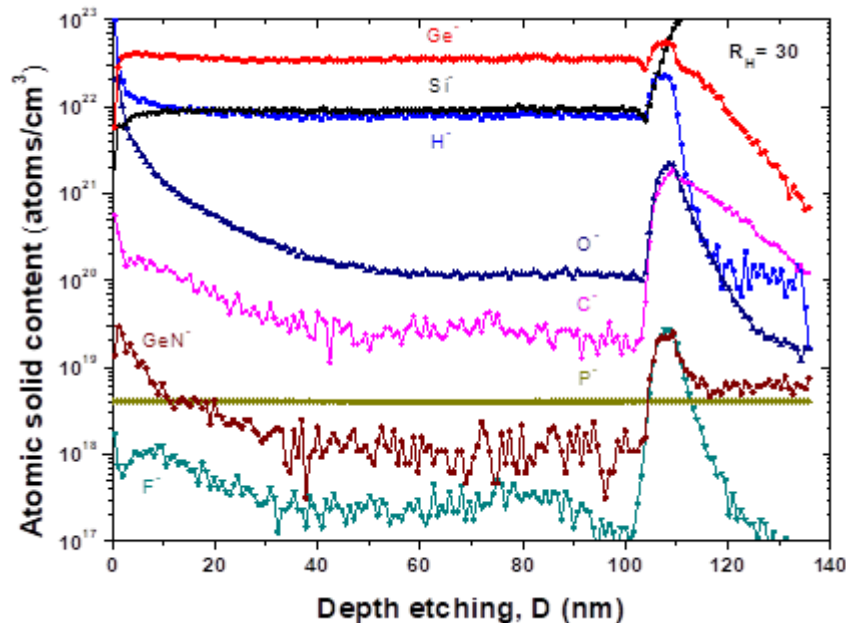

Figure 2. SIMS depth profile of H-, C-, O-, F-, Si-, P-, Ge-, GeN- elements in silicon–germanium film ($R_H = 30$) grown on p$^+$-doped c-Si wafer.

The relative contents of X, Y and Z elements as a function of R_H in $Si_X Ge_Y:H_Z$ are presented in Figure 3. Hydrogen content Z in the solid-state in the films decreases from Z = 0.24 to 0.15 when the dilution ratio increases from $R_H = 9$ to 30. Further H-dilution slightly changes the hydrogen content from Z = 0.15 to 0.175. This behavior together with almost constant values of X and Y in this region suggests that there is no change in hydrogen termination of both Si and Ge atoms in the films. Germanium content increases from Y = 0.485 to 0.70 as the dilution ratio increases from $R_H = 9$ to 30. In the range of $R_H = 30$ to 80, the germanium solid content is constant Y = 0.69 ± 0.01. Such behavior and the Y value differ from those in the films grown from LF discharge, in which Y has a constant value of 0.965 ± 0.005 in the entire reported range of $R_H = 20$ to 80. As it is depicted in Figure 3 higher dilution provides higher germanium and lower hydrogen content in comparison with that at low dilution, a similar result is reported in reference [10]. Silicon content decreases from X = 0.27 to 0.13 with R_H increase from $R_H = 9$ to $R_H = 40$ and then it remains at a constant value X = 0.137 ± 0.008 from $R_H = 40$ to 80.

Normalized solid component values of $Si_X Ge_Y:H_Z$ films and deposition rates as a function of hydrogen dilution are shown in Figure 4. The deposition rate $V_d(R_H)$ has similar behavior to that of the solid content of silicon, meaning that the deposition of the films is controlled by Si atom incorporation. If we compare $X(R_H)$ and $Y(R_H)$ with hydrogen behavior $Z(R_H)$ there would be a reason to suggest that hydrogen mostly terminates Si atoms in the entire studied R_H range. In other words, Ge atoms could be not sufficiently passivated by hydrogen which results in deterioration of the electronic properties. However, this suggestion is not supported by FTIR data. We continue the discussion of H-termination

in the section related to FTIR data analysis. This aspect has not been systematically reported and analyzed as yet in the literature.
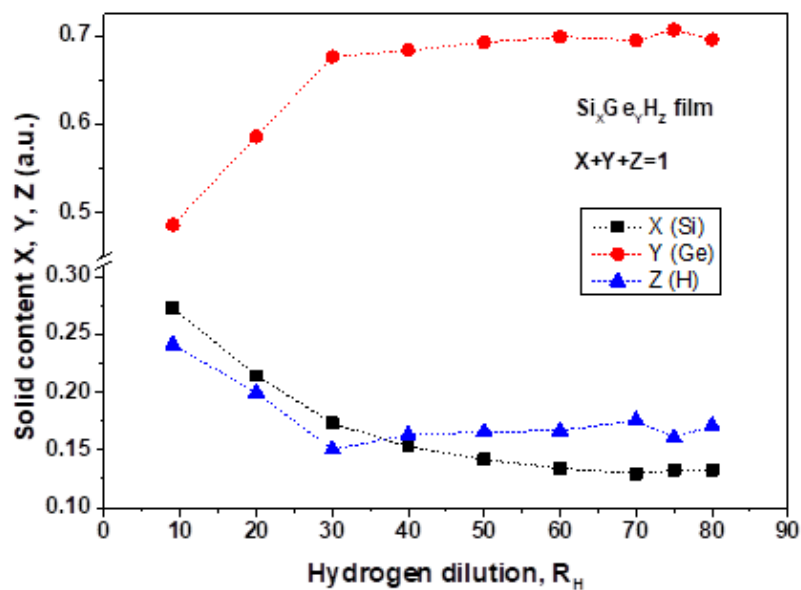

Figure 3. Solid content composition for $Si_X Ge_Y$:H_Z films as a function of the hydrogen dilution rate.

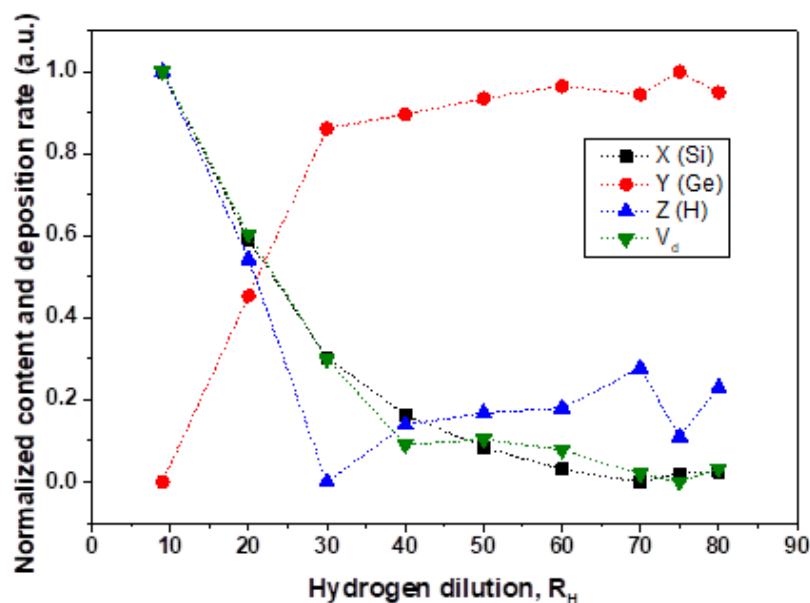**Figure 4.** Normalized values for solid silicon, germanium, and hydrogen content and deposition rate of $Si_X Ge_Y$:H_Z films as a function of hydrogen dilution ratio.

Incorporation of Ge atoms in Si–Ge:H film from the gas phase can be characterized by the coefficient of preferential incorporation (see e.g., [19]) defined as P_{Ge} = (relative Ge content in solid phase)/(relative content of Ge atoms in gas phase) and P_{Si} = (relative Si content in solid phase)/(relative content of Si atoms in gas phase). In the alloys, the relationship $P_{Ge} = 1/P_{Si}$ is evident. The coefficients of preferential incorporation, P_{Si}, and P_{Ge}, are shown in Figure 5. For P_{Ge} calculation the germanium content in the gas phase was $A = GeH_4/GeH_4 + SiH_4$ and solid content is represented by the $Si_{1-B}Ge_B$:H formula. This coefficient is conventionally obtained as the best fit parameter in experimental data processing for variation of composition within the entire range. Interestingly, many authors reported the best fit of their experimental data (obtained in very different conditions) with only one parameter (P_{Ge}) within the entire range of composition. Concrete P_{Ge} values were different depending on

deposition conditions. In this work, we calculated P_{Ge}, and P_{Si} for Ge–Si:H films deposited with different H-dilution in RF discharge.
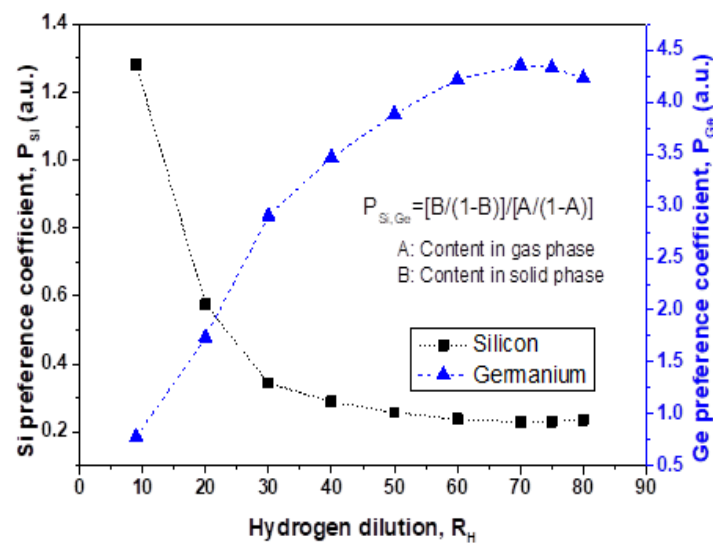

Figure 5. Coefficients of preferential incorporation of Si and Ge atoms, P_{Si} and P_{Ge}, as a function of hydrogen dilution.

Preferential incorporation strongly depends on hydrogen dilution in the range of R_H = 9 to 20 for silicon and R_H = 9 to 50 for germanium. For R_H = 20, P_{Ge} has a lower value of P_{Ge} = 1.73 in comparison with that reported for LF discharge (P_{Ge} = 6.44) [9]. For R_H = 9, P_{Ge} has a lower value of P_{Ge} = 0.78 in comparison with that reported for RF discharge (P_{Ge} = 6.1 and 4.6) [18]. The difference in P_{Ge} values could be attributed to differences in fabrication parameters. For example, power density in our experiments was w = 22 mW/cm^2 in comparison with w = 5 and 80 mW/cm^2 reported in [18] which provided P_{Ge} = 6.1 and 4.6, respectively. The latter P_{Ge} value is different from P_{Ge} = 12 found for SiGe:H films deposited at relatively high-power density (110 mW/cm^2) but low flow rate (7 sccm) and low dilution ratio (0.4) reported in [19]. Higher power densities provide the higher germanium content in the solid phase as shown in reference [10] for undiluted SiH$_4$ + GeH$_4$ mixtures; opposite behavior is observed for diluted mixtures. This data agrees with the high P_{Ge} > 1 value. From R_H = 60 to 80, P_{Ge} has a weak dependence on hydrogen dilution providing a value around P_{Ge} = 4.1 which is close to that discussed previously for RF discharge. In the case of other parameters such as deposition temperature or Ge content, there is no evidence of influence on P_{Ge} in the studied range [18].

3.3. H-Termination of Si and Ge Atoms

Hydrogen bonding with Si and Ge atoms was studied with FTIR spectroscopy. The general view of the FTIR spectrum is presented in Figure 6. Three groups of modes can be distinguished in the Figure: (1) Stretching mode for Si–H, Ge–H bonds (k = 1800–2200 cm^{-1}, (2) deformation modes for Si–H and Ge–H bonds (k = 500–700 cm^{-1}) and (3) Si–O and Ge–O bonds (k = 1000–1200 cm^{-1}, and k = 900–1000 cm^{-1}, respectively). We shall focus on the regions of stretching modes for Si–H and Ge–H bonds. For illustration, a fragment of the FTIR spectrum corresponding to Si–H and Ge–H modes is shown in Figure 7.

Both, the experimental data and results of the deconvolution are presented in this figure. In this, three peaks are observed around k ≈ 1880 cm^{-1}, k ≈ 2000 cm^{-1}, and k ≈ 2100 cm^{-1} assigned to Ge–H, Si–H, and Si–H$_2$ stretching modes, respectively. In Table A1, the peaks, contour width, and area are summarized. It is possible to observe in Table A1 that the hydrogen dilution changes remarkably these characteristics. Figure 8 shows the plot of the H-termination preference coefficients for Si–H and Ge–H bonds for different H-dilution, where $P_{Ge–H}$ = (relative Ge–H bonds content in solid phase)/(relative

content of Ge atoms in gas phase) and $P_{Si–H}$ = (relative Si–H bonds content in solid phase)/(relative content of Si atoms in gas phase); the relative contents were determinate from the IR stretching Ge–H (1880 cm^{-1}) and the Si–H (2000 cm^{-1}) absorption band integrated areas. The definition and explanation of P_{GeH} y P_{SiH} concepts are similar to P_{Ge} and P_{Si} gave in reference [19]. For low $R_H \leq 20$ the P_{SiH} decreases from 2.42 to 1.16 and P_{GeH} slightly increases from 0.42–0.57. In the range of $20 \leq R_H \leq 40$ the values are $P_{GeH} = P_{SiH} = 1$ (both values calculated from stretching modes), this means that the H termination for Si and Ge atoms is similar.

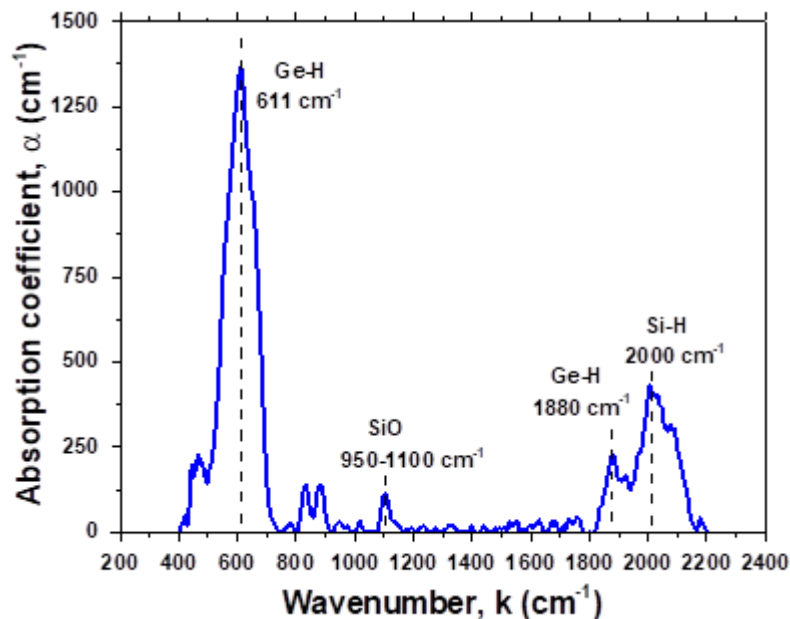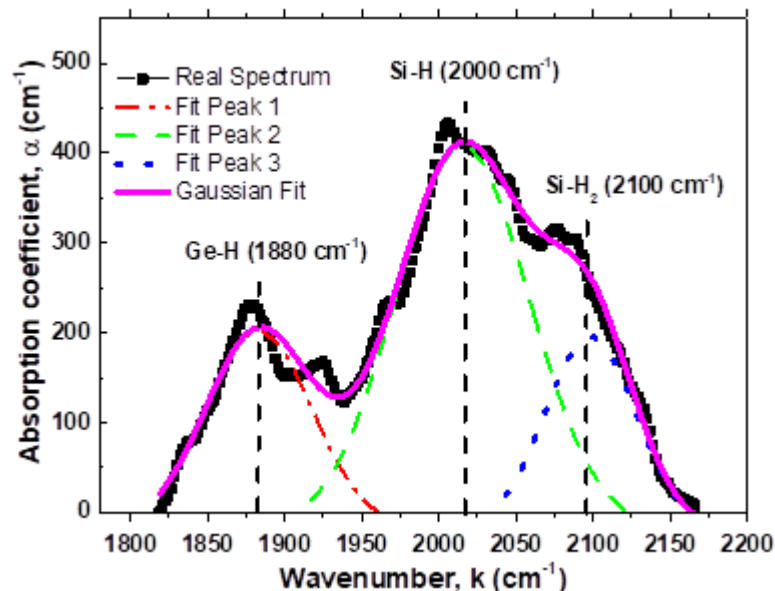**Figure 6.** General view of IR spectra in the Si–Ge:H samples deposited at $R_H = 0.9$.

Figure 7. Experimental IR spectrum of stretching vibration modes and deconvolution of Ge–H and Si–H for the SiGe:H films deposited at $R_H = 09$.

In the range $R_H \geq 40$, P_{GeH} increases to its maximum value $P_{GeH} = 4.3$ at $R_H = 75$ while P_{SiH} reduces to $P_{SiH} \approx 0.22$. It means that all Ge atoms have been mostly terminated by hydrogen in contrast to Si atoms. Thus we can clearly distinguish three regions: low $R_H \leq 20$, where Si atoms are preferentially terminated with hydrogen while Ge atoms have shortage of hydrogen, medium region

$20 \leq R_H \leq 40$ where H-termination starts to change (P_{SiH} reduces and P_{GeH} slightly increases), and finally the region of high dilution $R_H \geq 40$, where Ge atoms are mostly terminated by hydrogen but Si atoms do not have sufficient hydrogen. It would be reasonable to expect that for such "anti-correlation" between hydrogen terminations of Si and Ge atoms, for the low R_H region the defects expected would be due to Ge atoms not passivated by hydrogen. For a high level of H-dilution $R_H \geq 40$, Ge atoms are completely terminated with hydrogen, while Si atoms have not enough hydrogen passivation and therefore would reveal themselves as defects (e.g., dangling bonds).
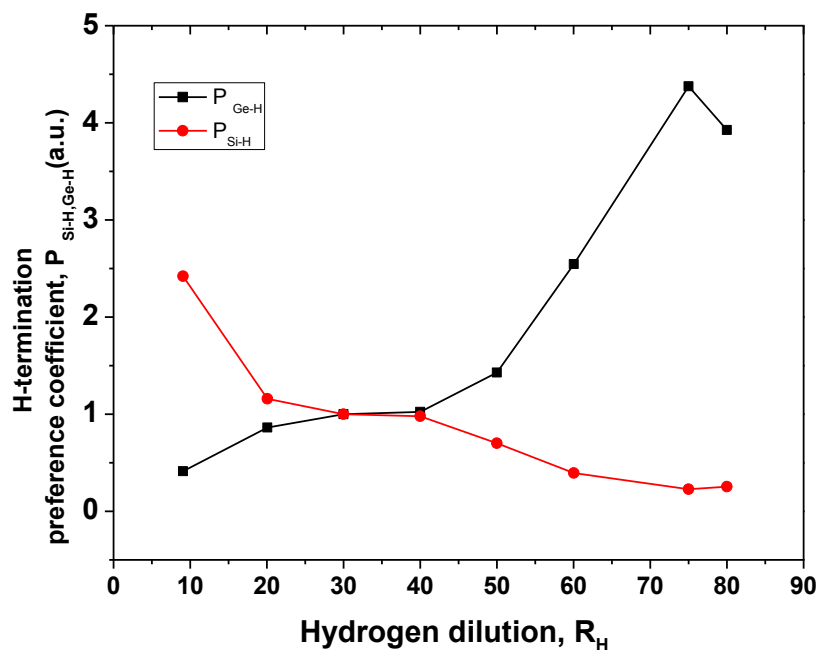

Figure 8. Factor of preferential H- termination for Si–H and Ge–H bonds in the Si–Ge:H films deposited with different H-dilution.

This next section is divided by subheadings. It provides a concise and precise description of the experimental results, their interpretation, as well as the experimental conclusions that can be drawn.

4. Discussion

4.1. Incorporation of Si, Ge in RF Versus LF PECVD

It is interesting to compare the growth rate of the films deposited with H-dilution. In reference [9] an increase in the growth rate is correlated with Ge content in both the gas phase and solid phase for Si-Ge films deposited with fixed H-dilution ($R_H = 20$). The films studied in [9] were deposited by low-frequency PECVD at fixed $R_H = 10$ with different Ge content in the gas. In this work, the films were grown by RF PECVD at low deposition temperature. The Ge relative content was equal to that of Si in the gas phase and both were fixed at the value 0.5 while R_H was varied. Thus, the conditions were different in this work and the reference [9]. If we compare the deposition rate observed in this work and that reported in [9] at "similar" $R_H = 20$, and relative Ge, Si content in gas phase 0.5, one can see that $V_d = 0.9$ A/s in this work (RF discharge) is less than $V_d = 2.3$ A/s (LF discharge) reported in [9]. However, this comparison does not allow the conclusion that the deposition rate in RF discharge is less than that in LF discharge due to the discharge power density in [9] where the LF discharge was remarkably higher (W = 120 mW/cm^2) than that in RF discharge (W = 22 mW/cm^2 in RF discharge). Additionally, the deposition temperature in [9] was higher ($T_d = 300$ °C) than the temperature used in this work ($T_d = 160$ °C). The deposition pressure is similar in both LF (P = 0.60 Torr) and RF (P = 0.55 Torr) experiments.

Preferential incorporation of Ge atoms was observed for film growth at $R_H = 20$ where the preferential factor for Ge was $P_{Ge} = 6.44$ even though the concentration of Ge and Si atoms was kept equal in the gas mixture. In this work, we observed also Ge preferential incorporation for $R_H > 15$ but the preferential factor changed with R_H from $P_{Ge} = 1.2$ at $R_H = 15$ to maximum $P_{Ge} = 4.2$ at $R_H = 75$. It is worth noting that despite the Ge preferential incorporation in the range of $15 < R_H < 80$, the growth rate (following the trend of the Si incorporation) and hydrogen content (determined by SIMS) suggest that the growth rate is determined by Si atoms incorporation.

Hydrogen content vs H dilution: If we compare hydrogen content versus H-dilution determined by SIMS presented in Figure 3, it shows a decrease from $[H]_{sims} = 0.25$ at $R_H = 10$ to $[H]_{sims} \approx 0.15$ at $R_H = 30$ and further, it stays constant with Si–H and Ge–H concentrations as a function of R_H. We can also see another trend: increasing of H bonded content with R_H with a maximum at $R_H = 70$. Taking into account that the SIMS signal is determined by both chemically bonded hydrogen and hydrogen absorbed (in pores and on surface) rather than only for chemically bonded hydrogen as is the case of FTIR measurements it is reasonable to suggest that with an increase of R_H, the total hydrogen content is reduced and the relative part of hydrogen-related to chemically bonded hydrogen is increased.

Let us compare our results on chemically bonded hydrogen distribution between Ge and Si atoms with those reported in the literature. In reference [9] the authors observed $P_{GeH} = 0.45, 0.61,$ and 0.29 in the films deposited with hydrogen ($R_H = 20$), argon dilution and without dilution in LF PECVD, respectively. Data obtained in this work in the range of $10 \leq R_H \leq 40$ in RF discharge $P_{GeH} \approx 0.5$ are in good agreement with those reported in [9]. However, we studied also the films deposited with higher values of R_H from 40 to 80 and we observed an increase of P_{GeH} to 3.2 at $R_H = 75-80$. Thus we demonstrated that it is possible to control both Ge content in the solid film (from $[Ge]_{sol} = 0.5$ to 0.7) and hydrogen termination of Si and Ge atoms (from $P_{GeH} = 0.5$ to $P_{GeH} = 3.2$) by varying hydrogen dilution R_H from 10 to 80.

4.2. Reduction of Vd and Preferential Solid Incorporation of Ge Atoms

Because the PECVD deposition of thin films is a complex process, the final characteristics of the films vary from system to system and growth conditions have interdependence from parameters such as power density, substrate temperature, chamber pressure, etc. In this section, we discuss only the results based on three general processes: (i) Gas/plasma phase process, (ii) species transport process to the surface and (iii) solid growth process on the surface. In (i), increasing R_H, while pressure and RF power are kept constant, means dilution of the silicon and germanium precursors decreasing the number of radicals available to be transported to the surface. Thus, V_d decreases with increase of R_H (Figure 4). On the other hand, the amount of hydrogen radicals is increased altering the reaction in the plasma. It is important to note that the binding energy of Ge–H (2.97 eV/bond) is lower than that of Si–H (3.2 eV/bond) [20], then, it is expected that decomposition of GeH_4 will be faster than SiH_4 and the Ge radicals will become an important factor for growth when both, silicon and germanium radicals are scarce. This explains the preferential solid incorporation of Ge atoms to the film when R_H is increased. In (ii), the sheath region of the glow discharge is responsible for transporting the species from plasma bulk to the film surface and this also results in ion bombardment. In consequence, the increase of R_H is expected to increase the number of H radicals for diffusion, sticking, and etching in (iii) [21], then the possible effects of hydrogen dilution include: (a) Etching of weak bonds with preferential etching of silicon over germanium atoms [22], (b) more hydrogen atoms sticking to superficial bonds decreasing the reactivity of the surface and (c) hydrogen atom diffusion into the bulk causing restructuration of the alloy network (for example, increasing the H termination). In this case, etching and sticking will contribute to the reduction of V_d and explain the preferential solid incorporation of Ge atoms in the solid phase (Figures 4 and 5).

4.3. Preferential Ge–H Termination

According to Section 4.1, the increase of hydrogen dilution enhances hydrogen termination on the surface but also increases the implantation of hydrogen atoms due to ion bombardment [21]. In this case, hydrogen radicals provide additional energy to activate the reaction of hydrogen with silicon and germanium atoms on the surface. This factor is mainly important if the deposition process is at low deposition temperatures (T_d < 200 °C). On the other hand, the increase of preferential termination of Ge atoms with the increase of hydrogen dilution is explained by a Ge-dominated surface where the reactions of hydrogen activation are concentrated. This Ge-dominated surface is the result of an increase of germanium in the solid/gas phase and preferential etching of silicon atoms [22]. The high rate of Ge–H termination in silicon-germanium thin films has a strong correlation to stability against light exposure. It is important to note, then, that an increase of H dilution increases the amount of Ge atoms terminated by hydrogen (Figure 8), but reduces the amount of hydrogen in the solid phases (Figure 4). This may due to the extra energy provided by ion bombardment of H radicals on the surface that also stimulates the local desorption of hydrogen.

5. Conclusions

The effect of H-dilution in the range of R_H = 10 to 80 on the composition and hydrogen termination of Si and Ge atoms in $Si_XGe_Y:H_Z$ films deposited by RF PECVD at low deposition temperature (T_d = 160 °C) was investigated. Incorporation of Si and Ge atoms from the gas phase into the solid films depended strongly on H-dilution: reducing for Si and increasing for Ge atoms with an increase of R_H from 10 to 30. Preferential incorporation increased for Ge atoms (P_{Ge}) and reduced for Si atoms (P_{Si}) with an increase of R_H. Maximum P_{Ge} = 4.2 is obtained in the films deposited at R_H = 70 while the maximum P_{Si} was P_{Si} = 1.3 at R_H = 10. This means that hydrogen dilution results in a significant increase of Ge atom incorporation.

H-termination of Si and Ge atoms studied by FTIR spectroscopy revealed that at low H-dilution (R_H = 10), hydrogen preferentially terminated Si atoms with a P_{SiH} = 3.2. Then in the range of 20 < R_H < 40, P_{SiH} decreases to the value P_{SiH} = 1.7. Further increase of H-dilution from R_H = 40 to 50 P_{SiH} results in a P_{SiH} = 0.5, staying without change up to R_H = 80. The H-termination of Ge atoms was practically not changed from the value R_{GeH} = 0.5 in the range of 10 < R_H < 40. Further increase of R_H from R_H = 40 to 80 resulted in an increase of P_{GeH} from 0.5 to 4.3 providing substantial preferential incorporation for Ge atoms (P_{GeH} = 4.3) in the films deposited at high hydrogen dilution (R_H = 80). From these observations and data analysis under the studied conditions we can draw the following conclusions:

(1) Dilution by hydrogen decreases the deposition rate due to factors such as the dilution of silicon and germanium precursors, etching of the silicon atoms, and reduction of the reactivity of the surface.

(2) For all films, preferential incorporation of Ge atoms (P_{Ge}) is observed. This may be associated with the lower binding energy of Ge–H (2.97 eV/bond) than that of Si–H (3.2 eV/bond) which results in more germanium precursors in the plasma. The lower preferential incorporation coefficient of silicon atoms can be explained by the preferential etching of silicon atoms due to an increase of hydrogen radicals.

(3) Hydrogen preferentially terminates Ge atoms with an increase of the hydrogen dilution as a consequence of an increase of Ge atoms in the solid phase on the surface and an increase of surface energy provided by the hydrogen radicals.

Conflicts of Interest: The authors declare no conflicts of interest. The funders had no role in the design of the study; in the collection, analyses, or interpretation of data; in the writing of the manuscript, or in the decision to publish the results.
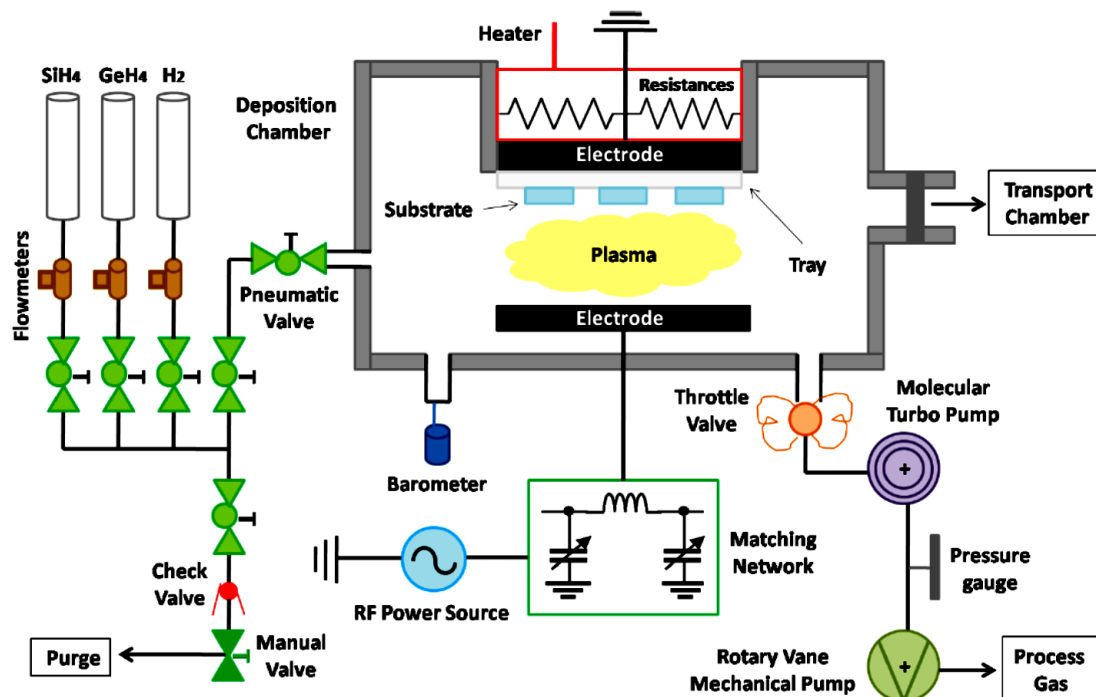
Appendix A

Figure A1. MVSystem Plasma Enhanced Chemical Vapor Deposition (PECVD) chamber configuration.

Appendix B

Table A1. Peak assignments in FTIR spectra of the films studied.

Sample	K [cm^{-1}]	W [cm^{-1}]	S [cm^{-2}]	Bonding (cm^{-1}) Ref. [23]
$R_H = 09$	608.2 ± 0.5	111 ± 1	$(1.50 \pm 0.03) \times 10^5$	Ge–H (570) and Si–H (630) bending
	1883.2 ± 0.9	81 ± 3	$(1.9 \pm 0.1) \times 10^4$	Ge–H (1880) stretching
	2015 ± 1	101 ± 3	$(4.6 \pm 0.2) \times 10^4$	Si–H (2000) stretching
	2098 ± 2	69 ± 4	$(1.5 \pm 0.2) \times 10^4$	SiH$_2$ (2090–2140) stretching
$R_H = 20$	570 ± 5	73 ± 6	$(4.9 \pm 0.8) \times 10^4$	Ge–H (570) bending
	616 ± 1	47 ± 5	$(3.5 \pm 0.9) \times 10^4$	Si–H (630) bending
	664 ± 1	41 ± 1	$(3.1 \pm 0.2) \times 10^4$	Si–H$_2$ (670) wagging or Si–C stretching
	1883.2 ± 0.8	86 ± 4	$(2.5 \pm 0.2) \times 10^4$	Ge–H (1880) stretching
	2013 ± 3	77 ± 4	$(2.9 \pm 0.2) \times 10^4$	Si–H (2000) stretching
	2089 ± 6	85 ± 13	$(1.5 \pm 0.4) \times 10^4$	SiH$_2$ (2090–2140) stretching
$R_H = 30$	559 ± 1	40 ± 2	$(1.9 \pm 0.3) \times 10^4$	Ge–H (570) bending
	608.2 ± 0.9	61 ± 5	$(5.3 \pm 0.4) \times 10^4$	Ge–H (570) and Si–H (630) bending
	666.9 ± 0.8	45 ± 1	$(3.8 \pm 0.2) \times 10^4$	Si–H$_2$ (670) wagging or Si–C stretching
	1878 ± 2	65 ± 3	$(3.9 \pm 0.3) \times 10^4$	Ge–H (1880) stretching
	2015 ± 1	67 ± 5	$(3.9 \pm 0.5) \times 10^4$	Si–H (2000) stretching
	2093 ± 5	93 ± 8	$(2.8 \pm 0.3) \times 10^4$	SiH$_2$ (2090–2140) stretching or SiH–O
$R_H = 40$	571 ± 5	68 ± 5	$(4.7 \pm 0.9) \times 10^4$	Ge–H (570) bending
	618 ± 2	54 ± 6	$(4 \pm 1) \times 10^4$	Ge–H (570) and Si–H (630) bending
	1873 ± 2	69 ± 7	$(4.5 \pm 0.8) \times 10^4$	Ge–H (1880) stretching
	2008 ± 1	64 ± 3	$(4.4 \pm 0.4) \times 10^4$	Si–H (2000) stretching
	2096 ± 2	91 ± 8	$(3.8 \pm 0.6) \times 10^4$	SiH$_2$ (2090–2140) stretching or SiH–O
$R_H = 50$	579.2 ± 0.5	71 ± 1	$(4.5 \pm 0.1973) \times 10^4$	Ge–H (570) bending
	667.3 ± 0.3	53.2 ± 0.9	$(5.6 \pm 0.1) \times 10^4$	Si–H$_2$ (670) wagging or Si–C
	1876.0 ± 0.2	18.2 ± 0.5	$(5.0 \pm 0.2) \times 10^3$	Ge–H (1880) stretching
	2002.1 ± 0.3	22.0 ± 0.8	$(3.5 \pm 0.1) \times 10^3$	Si–H (2000) stretching
	2030.2 ± 0.7	23 ± 1	$(1.8 \pm 0.1) \times 10^3$	GeH$_3$ (2050–2060) stretching

Table A1. *Cont.*

Sample	K [cm^{-1}]	W [cm^{-1}]	S [cm^{-2}]	Bonding (cm^{-1}) Ref. [23]
R$_H$ = 60	578.1 ± 0.9	92 ± 3	$(3.0 ± 0.2) × 10^4$	Ge–H (570) bending
	1875.2 ± 0.5	38 ± 1	$(1.45 ± 0.05) × 10^4$	Ge–H (1880) stretching
	2009 ± 1	33 ± 2	$(5.7 ± 0.6) × 10^3$	Si–H (2000) stretching
	2031.9 ± 0.7	17 ± 1	$(1.7 ± 0.3) × 10^3$	GeH$_3$ (2050–2060) stretching
	2066.1 ± 0.6	23 ± 2	$(1.5 ± 0.2) × 10^3$	GeH$_3$ (2050–2060) stretching
SiGe:H R$_H$ = 70	565.5 ± 0.9	43 ± 1	$(2.8 ± 0.1) × 10^4$	Ge–H (570) bending
	611.8 ± 0.5	40 ± 1	$(3.4 ± 0.1) × 10^4$	Si–H (630) bending
	667.6 ± 0.2	43.6 ± 0.6	$(6.3 ± 0.1) × 10^4$	Si–H$_2$ (670) wagging or Si–C stretching
	1877.6 ± 0.4	34 ± 2	$(1.9 ± 0.1) × 10^4$	Ge–H (1880) stretching
	2032.6 ± 0.5	55 ± 1	$(1.78 ± 0.09) × 10^4$	Si–H y GeH$_3$Stretching
	2130.3 ± 0.7	72 ± 2	$(2.2 ± 0.1) × 10^4$	SiH$_3$ (2120–2140)Bending
	2178 ± 1	15 ± 3	$(1.0 ± 0.2) × 10^3$	SiH-O$_2$ (2160) cluster
SiGe:H R$_H$ = 75	559 ± 1	46 ± 3	$(3.1 ± 0.2) × 10^4$	Ge–H (570) bending
	610 ± 0.8	44 ± 2	$(4.0 ± 0.2) × 10^4$	Si–H (630) bending
	666 ± 0.4	41 ± 1	$(4.9 ± 0.1) × 10^4$	Si–H$_2$ (670) wagging or Si–C stretching
	1879 ± 0.3	41.1 ± 0.9	$(2.17 ± 0.05) × 10^4$	Ge–H (1880) stretching
	2002.1 ± 0.6	23 ± 1	$(4.8 ± 0.4) × 10^3$	Si–H (2000) stretching
	2036.9 ± 0.5	33 ± 1	$(9.2 ± 0.5) × 10^3$	GeH$_3$ (2050–2060) stretching
	2089 ± 1	39 ± 5	$(4.0 ± 0.7) × 10^3$	SiH$_2$ (2090–2140) stretching
	2143 ± 1	42 ± 6	$(5.7 ± 0.8) × 10^3$	SiH$_3$ (2120–2140)Bending
	2179 ± 1	20 ± 3	$(2.0 ± 0.5) × 10^3$	SiH–O$_2$ (2160) cluster
SiGe:H R$_H$ = 80	560.9 ± 0.4	42 ± 1	$(2.9 ± 0.1) × 10^4$	Ge–H (570) bending
	611.4 ± 0.3	40.3 ± 0.9	$(3.8 ± 0.1) × 10^4$	Si–H (630) bending
	667.4 ± 0.3	36 ± 1	$(1.8 ± 1.2) × 10^4$	Si–H$_2$ (670) wagging or Si–C stretching
	1880.4 ± 0.4	41 ± 1	$(1.61 ± 0.04) × 10^4$	Ge–H (1880) stretching
	2000.2 ± 0.9	25 ± 2	$(4.1 ± 0.8) × 10^3$	Si–H (2000) stretching
	2037.7 ± 0.7	36 ± 3	$(8.7 ± 0.7) × 10^3$	GeH$_3$ (2050–2060) stretching
	2079 ± 1	26 ± 3	$(3.1 ± 0.7) × 10^3$	SiH$_2$ (2090–2140) stretching

References

1. Park, J.; Dao, V.A.; Kim, S.; Pham, D.P.; Kim, S.; Le, A.H.T.; Kang, J.; Yi, J. High Efficiency Inorganic/Inorganic Amorphous Silicon/Heterojunction Silicon Tandem Solar Cells. *Sci. Rep.* **2018**, *8*, 1–11. [CrossRef] [PubMed]
2. Ţălu, S. *Micro and Nanoscale Characterization of Three Dimensional Surfaces. Basics and Applications*, 2015th ed.; Napoca Star Publishing House: Cluj-Napoca, Romania, 2015.
3. Yu, Z.; Zhang, X.; Zhang, H.; Huang, Y.; Li, Y.; Zhang, X.; Gan, Z. Improved power conversion efficiency in radial junction thin film solar cells based on amorphous silicon germanium alloys. *J. Alloys Compd.* **2019**, *803*, 260–264. [CrossRef]
4. Ji, X.; Cheng, H.Y.; Grede, A.J.; Molina, A.; Talreja, D.; Mohney, S.E.; Giebink, N.C.; Badding, J.V.; Gopalan, V. Conformal coating of amorphous silicon and germanium by high pressure chemical vapor deposition for photovoltaic fabrics. *APL Mater.* **2018**, *6*, 046105. [CrossRef]
5. Jiménez, R.; Moreno, M.; Torres, A.; Rosales, P.; Sanz, M.T.; Ambrosio, R. Performance Characterization of Infrared Detectors Based on Polymorphous Silicon-Germanium (pm-Si x Ge 1−x:H) Thin Films Deposited at Low Temperature. *Phys. Status Solidi* **2018**, *215*, 1700736. [CrossRef]
6. Wang, Q.; Vogt, H. With PECVD Deposited Poly-SiGe and Poly-Ge Forming Contacts Between MEMS and Electronics. *J. Electron. Mater.* **2019**, *48*, 7360–7365. [CrossRef]
7. Huerta, F.L.; García, R.M.W.; González, L.G.; May, A.L.H.; Arriaga, W.C.; Vega, R.; Soto, E. Biocompatibility and surface properties of hydrogenated amorphous silicon-germanium thin films prepared by LF-PECVD. *IOP Conf. Ser. Mater. Sci. Eng.* **2019**, *628*, 012003. [CrossRef]
8. Shima, M.; Isomura, M.; Maruyama, E.; Okamoto, S.; Haku, H.; Wakisaka, K.; Kiyama, S.; Tsuda, S. Investigation of hydrogenated amorphous silicon germanium fabricated under high hydrogen dilution and low deposition temperature conditions for stable solar cells. *Jpn. J. Appl. Phys. Part 1 Regul. Pap. Short Notes Rev. Pap.* **1998**, *37*, 6322–6327. [CrossRef]
9. Kosarev, A.; Torres, A.; Hernandez, Y.; Ambrosio, R.; Zuniga, C.; Felter, T.E.; Asomoza, R.; Kudriavtsev, Y.; Silva-Gonzalez, R.; Gomez-Barojas, E.; et al. Abramov, Silicon-germanium films deposited by low-frequency plasma-enhanced chemical vapor deposition: Effect of H 2 and Ar dilution. *J. Mater. Res.* **2006**, *21*, 88–104. [CrossRef]
10. Shima, M.; Terakawa, A.; Isomura, M.; Haku, H.; Tanaka, M.; Wakisaka, K.; Kiyama, S.; Tsuda, S. Effects of very high hydrogen dilution at low temperature on hydrogenated amorphous silicon germanium. *J. Non Cryst. Solids* **1998**, *227*, 442–446. [CrossRef]

11. MacKenzie, K.D.; Eggert, J.R.; Leopold, D.J.; Li, Y.M.; Lin, S.; Paul, W. Structural, electrical, and optical properties of a-Si1-xGex:H and an inferred electronic band structure. *Phys. Rev. B* **1985**, *31*, 2198–2212. [CrossRef] [PubMed]

12. Liu, Y.; Dalal, V.L. Properties of amorphous silicon-germanium films and devices deposited at higher growth rates. *MRS Proc.* **2002**, *715*, A18.3. [CrossRef]

13. Wickboldt, P.; Pang, D.; Paul, W.; Chen, J.H.; Zhong, F.; Chen, C.-C.; Cohen, J.D.; Williamson, D.L. High performance glow discharge a-Si−xGex:H of large x. *J. Appl. Phys.* **1997**, *81*, 6252–6267. [CrossRef]

14. Sahli, F.; Werner, J.; Kamino, B.A.; Bräuninger, M.; Monnard, R.; Paviet-Salomon, B.; Barraud, L.; Ding, L.; Leon, J.J.D.; Sacchetto, D.; et al. Fully textured monolithic perovskite/silicon tandem solar cells with 25.2% power conversion efficiency. *Nat. Mater.* **2018**, *17*, 820–826. [CrossRef] [PubMed]

15. Cosme, I.; Kosarev, A.; Mansurova, S.; Olivares, A.J.; Martinez, H.E.; Itzmoyotl, A. Hybrid photovoltaic structures based on amorphous silicon and P3HT: PCBM/PEDOT:PSS polymer semiconductors. *Org. Electron. Phys. Mater. Appl.* **2016**, *38*, 271–277. [CrossRef]

16. Madaka, R.; Kanneboina, V.; Agarwal, P. Low-Temperature Growth of Amorphous Silicon Films and Direct Fabrication of Solar Cells on Flexible Polyimide and Photo-Paper Substrates. *J. Electron. Mater.* **2018**, *47*, 4710–4720. [CrossRef]

17. Mansurova, S.; Cosme, I.; Kosarev, A.; Olivares, A.J.; Ospina, C.; Martinez, H.E. AZO/PEDOT: PSS Polymer Frontal Interface Deposited on Flexible Substrates for a-Si:H Photovoltaic Applications. *Polymers* **2018**, *10*, 1068. [CrossRef] [PubMed]

18. Stutzmann, M.; Street, R.A.; Tsai, C.C.; Boyce, J.B.; Ready, S.E. Structural, optical, and spin properties of hydrogenated amorphous silicon-germanium alloys. *J. Appl. Phys.* **1989**, *66*, 569–592. [CrossRef]

19. Chou, Y.-P.; Lee, S.-C. Structural, optical, and electrical properties of hydrogenated amorphous silicon germanium alloys. *J. Appl. Phys.* **1998**, *83*, 4111–4123. [CrossRef]

20. Shah, A.V. *Thin-Film Silicon Solar Cells*, 1st ed.; EPFL Press: New York, NY, USA, 2010. [CrossRef]

21. Martirosyan, V. Atomistic Simulations of H2 and He Plasmas Modification of Thin-Films Materials for Advanced Etch., Université Grenoble Alpes. Available online: https://tel.archives-ouvertes.fr/tel01803013/document (accessed on 15 January 2020).

22. Kim, S.; Park, C.; Lee, J.-C.; Cho, J.-S.; Kim, Y. Preferential etching of Si–Si bond in the microcrystalline silicon germanium. *Curr. Appl. Phys.* **2013**, *13*, 457–460. [CrossRef]

23. Collins, R.W. Hydrogenated amorphous silicon alloy deposition processes. *J. Non Cryst. Solids* **1994**, *170*, 210–213. [CrossRef]